Increased IL-12 inhibits B cells' differentiation to germinal center cells and promotes differentiation to short-lived plasmablasts

Sun Jung Kim,[1] Michele Caton,[2] Chuansheng Wang,[1] Magi Khalil,[1] Zhi-Jie Zhou,[1] John Hardin,[1] and Betty Diamond[1,2]

[1]Autoimmune Disease Laboratory, Feinstein Institute for Medical Research, Manhasset, NY 11030
[2]Department of Microbiology and Immunology, Albert Einstein College of Medicine, Bronx, NY 10461

B cells activated by antigen in T cell–dependent immune responses can become short-lived plasma cells, which remain in the spleen, or germinal center–derived memory or plasma cells, which show evidence of affinity maturation and, in the case of plasma cells, migrate to the bone marrow. We show that this cell fate decision can be governed by the cytokine environment engendered by activated dendritic cells (DCs). DCs from mice lacking the Fc receptor γ chain exhibited an activated phenotype in vitro. They secreted more of the proinflammatory cytokine IL-12, which led to the preferential generation of short-lived splenic plasma cells, with ensuing low affinity antibodies and a diminished recall response. Understanding the factors that regulate antigen-activated B cell differentiation and memory cell formation has implications for both antibody-mediated autoimmune disease and protective antibody responses.

CORRESPONDENCE
Betty Diamond:
bdiamond@nshs.edu

Abbreviations used: AID, activation-induced cytidine deaminase; BMDC, BM-derived DC; dsDNA, double-stranded DNA; MAP, multiple antigenic peptide.

B cells responding to antigen in a T cell–dependent response can be activated to become short-lived plasma cells with no memory capabilities, or germinal center cells, which mature to become either long-lived plasma cells or memory B cells. The nature of the antibody-producing cell influences the duration of the antibody response as well as the affinity and isotype of the antibody that is made, all of which constitute important parameters of protective immunity. The phenotype of the autoreactive B cell producing the autoantibody in patients with autoimmune disease may also influence both the pathogenicity of the autoantibody and the response to therapy. Antibody responses that include a memory cell compartment may be important in protective immunity, but as autoantibody responses they may be more difficult to eradicate. Thus, understanding the conditions that lead to the generation of either short-lived plasma cells or long-lived plasma cells and memory cells may be of considerable clinical importance.

We have previously described a model of antigen-induced autoimmunity in which we can

examine the inductive phase of the autoreactive humoral response. BALB/c mice immunized with a peptide mimotope of double-stranded DNA (dsDNA) will develop antibodies that are cross-reactive with dsDNA and peptide. These antibodies deposit in renal glomeruli and cause proteinuria. Because there is minimal cellular infiltrate in the kidney, probably because of a lack of renal vulnerability to antibody-mediated disease in this strain, the model is one of nephrotic syndrome (1). The autoantibody response in these mice is T cell–dependent, with antigen-specific T cells producing Th1 cytokines on antigen challenge (2).

Our understanding of the immunological function of γ chain–associated FcRs has been facilitated by studies from Takai et al. (3) on FcR-associated γ chain–null mice (Fcγ$^{-/-}$). The Fcγ$^{-/-}$ mice have a selective defect in the expression of FcRs on the cell surface as well as in the FcR-mediated signal cascade. Interestingly, disruption of the FcR γ chain in NZB/

S.J. Kim and M. Caton contributed equally to this paper.
The online version of this article contains supplemental material.

NZW mice uncouples immune complex formation from the inflammatory response in the kidney, implying a pathogenic role of FcR γ chain in autoimmune disease (4).

There are several factors involved in determining the phenotype of antigen-experienced B cells, including BCR signal strength (5), expression of transcription factors (6), and costimulatory influences (7–9). In the course of studying renal pathology in peptide-immunized mice deficient in the FcR γ chain ($Fc\gamma^{-/-}$), we made the surprising observation that $Fc\gamma^{-/-}$ mice preferentially develop short-lived plasma cells and fail to develop a germinal center response. We show that this altered B cell response is a consequence of increased IL-12 production by DCs.

RESULTS

$Fc\gamma^{-/-}$ mice display a distinct humoral response to antigen

Immunization of BALB/c mice with a peptide mimotope of dsDNA, DWEYSVWLSN, octamerized on a polylysine backbone (multiple antigenic peptide [MAP] peptide) induces antibodies that cross-react with peptide and dsDNA (1). We immunized $Fc\gamma^{-/-}$ and WT mice i.p. with MAP peptide in CFA and boosted with antigen in IFA on days 7 and 14. By day 28, $Fc\gamma^{-/-}$ mice generated significantly higher serum titers of both antipeptide (approximately fivefold) and anti-dsDNA antibody (approximately sevenfold; Fig. 1 a). The difference in serum antibody reactivity did not reflect a difference in the kinetics of the response, as both strains exhibited a similar timing of antibody production (Fig. 1 a). An antigen-specific IgM response was induced in WT and $Fc\gamma^{-/-}$ mice. Consistent with the IgG response, there was a higher IgM response in $Fc\gamma^{-/-}$ mice at week 2, but this declined to the basal level by week 4 in both strains (Fig. S1, available at http://www.jem.org/cgi/content/full/jem.20070731/DC1).

One explanation for the greater IgG serum reactivity in $Fc\gamma^{-/-}$ mice would be an increased affinity of antipeptide antibodies. We, therefore, performed inhibition ELISAs with soluble peptide and calculated apparent affinities by determining the molar concentration of soluble antigen that led to 50% inhibition of the antibody reactivity (10). Contrary to our initial expectation, antipeptide antibodies from $Fc\gamma^{-/-}$ mice had a log lower apparent affinity than antipeptide antibodies from WT mice (1.4×10^5 vs. 2.2×10^6; $P \leq 0.01$), demonstrating that the increased titers resulted from the production of more antigen-specific antibody.

Furthermore, although IgG1 was the predominant isotype observed in both the antipeptide and anti-dsDNA response in WT mice, $Fc\gamma^{-/-}$ mice produced both IgG1 and IgG2a antipeptide (Fig. 1 b) and anti-dsDNA antibodies (not depicted). This did not reflect an intrinsic bias toward increased IgG2a, as the isotype distribution for total serum IgG was similar in both mouse strains (not depicted).

Because the difference in antibody titer between strains was ~5–10-fold, we believed it was important to ask whether this increase in serum antibody titer might be of pathological significance. Kidneys from MAP peptide–immunized $Fc\gamma^{-/-}$ mice, analyzed 13 wk after the initial antigen challenge, had

significantly more glomerular IgG deposition than WT kidneys, and the mice displayed increased proteinuria (Fig. 1 c). Thus, the antibodies from $Fc\gamma^{-/-}$ mice, although of lower affinity than the antibodies in WT mice, were still of sufficient affinity to cause glomerular dysfunction. This observation is
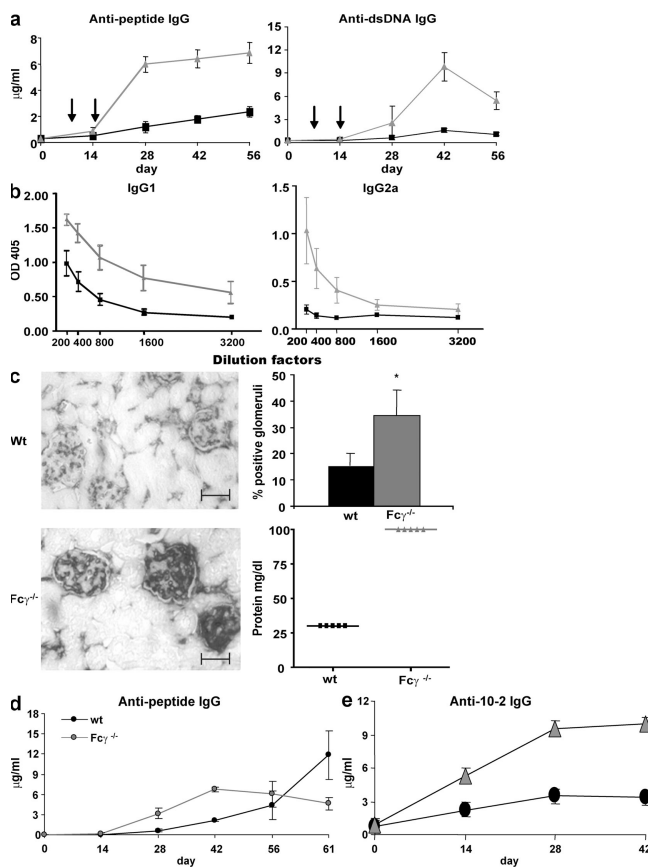

Figure 1. $Fc\gamma^{-/-}$ **mice display an increased production of antigen-specific antibodies in their serum and increased renal antibody deposition.** (a) $Fc\gamma^{-/-}$ (gray triangles) and WT (black squares) mice ($n = 5$ in each group) were immunized with 100 μg MAP peptide and boosted twice (arrows indicate time of boosts). Serum was collected on days 0, 14, 28, 42, and 56, and antipeptide and anti-dsDNA IgG ELISAs were performed. $P \leq 0.05$ in both graphs. (b) Mice were immunized as described in a. 7-wk serum was assayed for isotype-specific antipeptide antibody ELISAs. Titrations were twofold and began at the dilution indicated on the x-axis. Gray triangles show $Fc\gamma^{-/-}$ mice and black squares show WT mice. IgG1, $P = 0.02$; IgG2a, $P = 0.048$. $n = 5$. (c) Kidneys were taken at day 91, and sections were stained for IgG deposition. Sections shown above are representative of five mice in each group. Sections were magnified 100×. Bars, 50 μm. 50 glomeruli were counted in each kidney section, and the percent positive for IgG deposition was graphed. *, $P \leq 0.05$. Proteinuria was determined by measuring the amount of protein in the urine of mice at day 91 after immunization. (d) Both WT and $Fc\gamma^{-/-}$ mice were immunized with 100 μg MAP peptide in CFA on day 0 and boosted on day 7 with MAP peptide in IFA. On day 56, mice were challenged with 100 μg MAP peptide in IFA, and serum was collected 5 d after challenge. Antipeptide ELISAs were performed. $P \leq 0.05$. (e) WT and $Fc\gamma^{-/-}$ mice (five in each group) were immunized with 100 μg 10–2–BSA and boosted twice. Day-0, -14, -28, and -42 serum was assayed by ELISA for anti-10-2 IgG. $P \leq 0.05$. Data are presented as mean ± SD.

consistent with clinical experience where a four- to eightfold increase in autoantibody titer may correlate with the onset of disease or with increased disease activity. For example, an antinuclear antibody titer of 1:40 is normal, whereas an eightfold increase to 1:320 is highly significant for disease. Likewise, a four to eightfold increase in anti-DNA antibody titer in a patient with SLE will often precede a clinical flare (11).

High affinity antibody responses are generated by a germinal center reaction in which B cells undergo somatic hypermutation and there is selection for survival of B cells making the highest affinity antibodies. These cells mature to become long-lived plasma cells and memory cells. To determine if the lack of a high affinity antibody response reflected a failure of B cells to undergo germinal center maturation, we questioned whether $Fc\gamma^{-/-}$ mice developed a memory response. WT and $Fc\gamma^{-/-}$ mice were immunized and boosted with MAP peptide. 8 wk later, mice were challenged with 100 µg MAP peptide. 5 d later, blood was collected to measure the antipeptide response in serum. Fig. 1 d shows that WT mice have a rapid increase in the serum antipeptide response, which was not observed in $Fc\gamma^{-/-}$ mice. These data suggest a significant reduction in the population of memory B cells in $Fc\gamma^{-/-}$ mice.

To determine whether $Fc\gamma^{-/-}$ mice immunized with a nonself antigen would also develop an enhanced serum response, we examined the response of $Fc\gamma^{-/-}$ mice to 10–2, a peptide mimotope of phosphorylcholine, conjugated to BSA (12). As seen in Fig. 1 e, $Fc\gamma^{-/-}$ mice made significantly more anti–10-2 antibodies (an approximately threefold increase in titer) than WT mice. In addition, although WT mice made predominantly IgG1 anti–10-2 antibodies, $Fc\gamma^{-/-}$ mice also produced antigen-specific IgG2a antibodies (unpublished data). Thus, the strain-specific difference in antibody response was not limited to an autoreactive response.
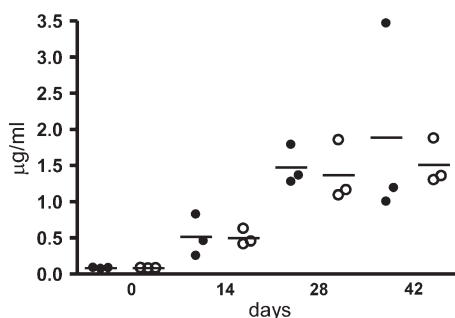

Figure 2. Antipeptide response of muMT mice reconstituted with either WT B cells or $Fc\gamma^{-/-}$ B cells. Spleens were taken from 6–8-wk-old WT and $Fc\gamma^{-/-}$ mice. B cells were purified as described in Materials and methods, and 2×10^7 total B cells were adoptively transferred to muMT mice i.v. After 2 wk, muMT mice with WT B cells or $Fc\gamma^{-/-}$ B cells were immunized with 100 µg MAP peptide as described. Blood was collected on days 0, 14, 28, and 42, and the antipeptide antibody was measured by ELISA. Closed circles, muMT mice with WT B cells; open circles, muMT mice with $Fc\gamma^{-/-}$ B cells. Each circle represents an individual mouse, and the horizontal bar is the mean.

Differential humoral response in $Fc\gamma^{-/-}$ mice is not determined by B cells

The increased antipeptide and anti-DNA response in $Fc\gamma^{-/-}$ mice might reflect either a B cell–intrinsic phenotype or, alternatively, a different response to immunization in non-B cells. To test whether the difference was B cell intrinsic, splenic B cells from WT or $Fc\gamma^{-/-}$ mice were transferred to B cell–deficient BALB/c mice (muMT). Both WT B cell–reconstituted and $Fc\gamma^{-/-}$ B cell–reconstituted muMT mice were immunized with MAP peptide. As shown in Fig. 2, there was no statistically significant difference in serum antipeptide response between WT and $Fc\gamma^{-/-}$ B cell–reconstituted mice. Moreover, analysis of splenic B cell subsets (mature vs. immature and transitional vs. follicular vs. marginal zone) confirmed that there was no difference in B cell differentiation between $Fc\gamma^{-/-}$ and WT BALB/c B cells. The expression of several cell surface markers (CD22, CD40, CD43, CD79b, CD27, MHC II, Fas, CD80, and CD86) also was not different between $Fc\gamma^{-/-}$ and WT BALB/c B cells. B cell function, assayed by IgM-mediated apoptosis and B cell proliferation to anti-IgM plus anti-CD40 antibody or anti-CD40 antibody plus IL-4, was also similar between both strains (unpublished data). Thus, the phenotype and function of naive B cells of both strains were indistinguishable.

$Fc\gamma^{-/-}$ B cells preferentially differentiate into short–lived plasma cells

Because the antibody response in $Fc\gamma^{-/-}$ mice was of low affinity and the memory response was impaired, we hypothesized that there was a defect in germinal center maturation, which generates both memory B cells and long-lived plasma cells, and a preferential generation of short-lived plasma cells (13–16). Short-lived plasma cells develop in T cell–dependent responses but do not display affinity maturation and are not associated with a clonally related memory B cell population (17, 18). After activation with antigen, short-lived plasma cells reside primarily in the extrafollicular foci of the spleen, whereas long-lived plasma cells preferentially migrate to the BM (16–19). First, we determined the number of antibody-secreting cells (including plasmablasts, short-lived plasma cells, and long-lived plasma cells) in the spleen. There was a higher percentage of B220^{lo} and CD138$^+$ cells in the B cell population in MAP peptide–immunized $Fc\gamma^{-/-}$ mice compared with WT mice on day 8 (Fig. 3 a). To determine the location of B220^{lo} and CD138$^+$ cells within the spleen, immunohistochemistry was performed on spleens of immunized mice. The majority of CD138$^+$ cells were positioned outside the B cell follicles where short-lived plasma cells reside (Fig. 3 b). CD138$^+$ cells colocalized with kappa chain positivity but not with CD4 positivity (unpublished data). To confirm this observation, we also performed peptide-specific ELISPOT assays of splenic B cells. Fig. 3 c shows that 2.5-fold more cells secreting specific antibody were present in spleens of $Fc\gamma^{-/-}$ mice than in WT spleens. By day 28, splenic plasma cells from both $Fc\gamma^{-/-}$ and WT mice declined in number, presumably because of apoptosis of short-lived plasma cells.
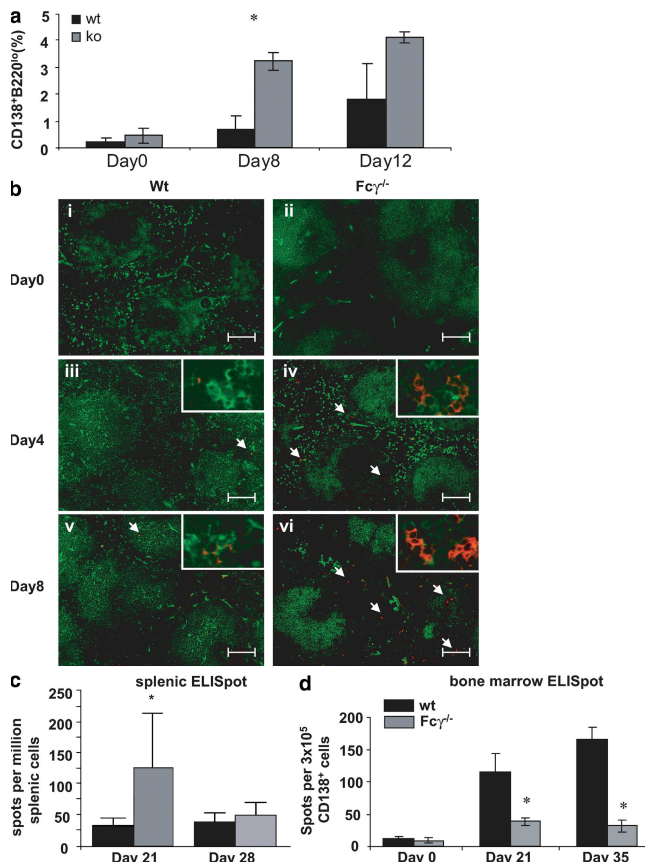
a

CD138+B220lo(%)

wt
ko

*

Day0   Day8   Day12

b

Wt   Fcγ-/-

Day0   i   ii

Day4   iii   iv

Day8   v   vi

c splenic ELISpot

spots per million splenic cells

*

Day 21   Day 28

d bone marrow ELISpot

wt
Fcγ-/-

Spots per 3x10^5 CD138+ cells

*   *

Day 0   Day 21   Day 35

Figure 3. Immunized Fcγ$^{-/-}$ mice have increased numbers of plasma cells in their spleen and decreased numbers in their BM compared with WT mice. (a) Spleens were taken from WT and Fcγ$^{-/-}$ mice on days 0, 8, and 12 after immunization, and splenocytes were stained with PE-conjugated goat anti–mouse CD138 and FITC-conjugated goat anti–mouse B220. The percentage of cells that were CD138$^+$ and B220^{lo} was analyzed by FlowJo software. Mean ± SD of two independent experiments is shown, and each experiment contained pooled cells from three mice. (b) Spleens were taken at days 0, 4, and 8 after immunization, and frozen tissue sections were incubated with anti–B220-FITC (green) and anti–CD138-PE (red). Results are representative of at least three mice per group. Images are magnified 10× and insets are 40×. Arrows indicate the position of CD138$^+$B220^{lo} cells. Bars, 100 μm. (c) Antipeptide ELISPOTs were performed on splenocytes taken on day 21 after immunization. Fcγ$^{-/-}$ mice are shown in gray and WT mice are shown in black. There were five mice in each group. P ≤ 0.05. Data are mean ± SD. (d) BM was obtained on days 21 and 35 after primary immunization. CD138$^+$ cells were purified by sorting. An equal number of CD138$^+$ cells from each strain were plated for an antipeptide ELISPOT assay. The number of spots was counted and total number of antipeptide antibody secreting cells was enumerated (mean ± SD of four mice). *, P ≤ 0.05.

Long-lived plasma cells migrate to the BM, where they secrete antibody. To determine whether long-lived plasma cells were being generated in Fcγ$^{-/-}$ mice, we enumerated plasma cells by peptide-specific ELISPOT assays in the BM. Plasma cells were detectable in the BM between days 21 and 35 after the initial immunization. Fcγ$^{-/-}$ mice had 5.3-fold fewer peptide-specific plasma cells in the BM on day 35 (Fig. 3 d).

These results were consistent with the preferential generation of short-lived plasma cells in Fcγ$^{-/-}$ mice in contrast to the predominance of long-lived plasma cells present in the BM of WT mice.

Because the antipeptide antibody response was previously shown to be a T cell–dependent response in WT mice (2), we questioned whether the antibody response in Fcγ$^{-/-}$ mice was also T cell dependent, as it displayed less evidence of germinal center formation. Fig. 4 a shows that antibody generation is abolished in CD4 T cell–depleted mice. Thus, the diminished germinal center response is not caused by an absent T cell response.

Antigen-specific T cells are activated by MAP peptide immunization in Fcγ$^{-/-}$ mice. To demonstrate T cell activation in Fcγ$^{-/-}$ mice, we assessed antigen-specific proliferation of T cells from MAP peptide–immunized mice. T cells from MAP peptide–immunized Fcγ$^{-/-}$ and WT mice proliferated in response to antigen (Fig. 4 b). In fact, the response of T cells from Fcγ$^{-/-}$ T cells was greater than that of WT T cells. To ascertain whether this enhanced T cell response reflected a change in T cell repertoire, we assessed Vβ usage. Fig. 4 c shows that there was no significant difference in TCR Vβ chain usage between WT and Fcγ$^{-/-}$ mice, either before or after MAP peptide immunization. Furthermore, antigen-specific T cells from both strains produced IL-2 and IFN-γ (unpublished data). These data demonstrate that T cells in Fcγ$^{-/-}$ mice were activated to at least the same extent as T cells from WT mice after MAP peptide immunization. Thus, the altered antibody response is not a consequence of a failure of T cell priming.

Fcγ$^{-/-}$ mice display a diminished germinal center response

To demonstrate directly that Fcγ$^{-/-}$ mice display reduced germinal center maturation of B cells, we asked whether the reduced affinity of serum antibodies in Fcγ$^{-/-}$ mice reflected a relative lack of somatic hypermutation occurring in the Fcγ$^{-/-}$ mice, as somatic hypermutation is a feature of the germinal center response and a critical contribution to affinity maturation. To address this question, we generated antigen-specific hybridomas from WT and Fcγ$^{-/-}$ mice immunized with MAP peptide. We examined the number of mutations in the region downstream of the rearranged J$_H$ in B cells making antipeptide antibody. We chose to enumerate mutations in this region because it has been shown to undergo hypermutation. Because it is not a coding region, it is not subject to the pressures of selection. As seen in Fig. 5 a, hybridomas from Fcγ$^{-/-}$ mice had many fewer mutations. Splenic histology displayed fewer germinal centers in Fcγ$^{-/-}$ mice after immunization (Fig. 5 b). This was confirmed by quantification of B220$^+$ PNA$^+$ cells in the spleen (Table S1, available at http://www.jem.org/cgi/content/full/jem.20070731/DC1). There were very few PNA$^+$ cells in the B220$^+$ population in Fcγ$^{-/-}$ mice on days 8 and 16 after immunization compared with WT mice (Fig. 5 c). We also measured activation-induced cytidine deaminase (AID) induction in germinal center B lymphocytes because expression
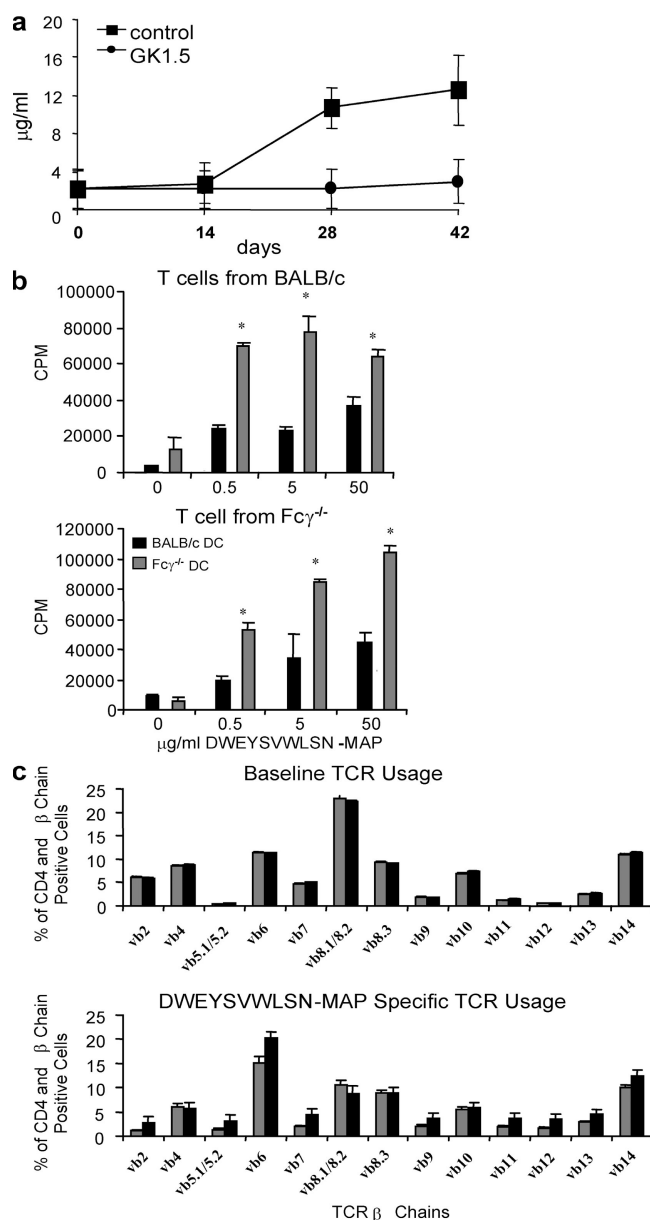
Figure 4. The antipeptide response in Fcγ$^{-/-}$ is T cell dependent. (a) Fcγ$^{-/-}$ mice were injected i.p. with 500 μg GK1.5 mAb (circles) or saline (squares) on days −1, 0, and +1. All mice were immunized, boosted with 100 μg MAP peptide, and boosted as described in Materials and methods (arrows indicate time of boost). Serum was collected on days 0, 14, 28, and 42, and an antipeptide ELISA was performed. *, P ≤ 0.05 (n = 3). (b) 10^5 BMDCs were pulsed with MAP peptide and cultured with T cells from MAP peptide–immunized WT or Fcγ$^{-/-}$ mice in a 1:1 (BMDC/T) ratio. 3 d later, ^{3}H-thymidine was added and incorporated thymidine was measured. *, P ≤ 0.05. These results are representative of three independent experiments. (c) Vβ usage was measured in WT and Fcγ$^{-/-}$ mice. T cells were harvested from naive and MAP peptide–immunized WT and Fcγ$^{-/-}$ mice as described in Materials and methods. T cells were incubated with peptide in vitro for 14 d. Naive and cultured CD4$^+$ T cells were stained with fluorochrome-labeled anti-Vβ chain antibodies. CD4 T cells expressing particular Vβ chains were analyzed by FlowJo software. Data are presented as mean ± SD.

of AID is suppressed in mature B cells and only expressed in germinal center B cells (20). WT mice display a significant induction of AID in germinal center B cells. Fcγ$^{-/-}$ mice, however, did not show any significant induction of AID, which is consistent with a diminished germinal center reaction in these mice (Fig. 5 d). These studies all support a reduced germinal center response in Fcγ$^{-/-}$ mice.

Fcγ$^{-/-}$ DCs have increased IL-12 production and an increased ability to cause B cell proliferation in an IL-12–dependent manner

Vogel et al. (21) showed that IL-12 can bind directly to B cells and induce plasma cell formation, and Dubois et al. (22, 23)
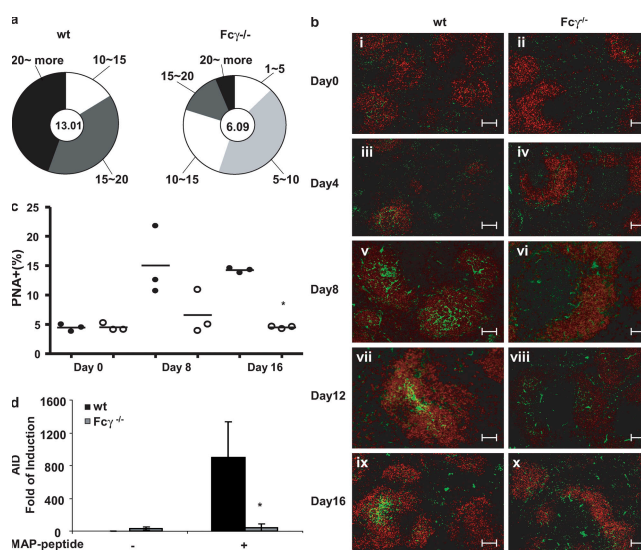

Figure 5. Fcγ$^{-/-}$ mice display a diminished germinal center response. (a) The JH2 to JH4 region was sequenced in MAP peptide–immunized mice (three mice in each group). Charts depict the mean mutation frequencies (frequency is defined as mutations per base pair sequenced × 10^{-3}) for the hybridoma clones that were sequenced (center of pie) and the proportion of sequences with mutations (numbers of mutations outside the pie slice). (b) Representative images of spleen sections from immunized WT and Fcγ$^{-/-}$ mice. Spleens were obtained on each designated day after immunization protocol and frozen for staining. Sections were stained with B cell–specific antibody B220-PE (red) and with germinal center marker PNA-FITC (green; three mice in each group). Bars, 100 μm. (c) Enumeration of PNA$^+$ B cells. Spleens were collected from WT and Fcγ$^{-/-}$ mice on days 0, 8, and 16 after immunization. Splenocytes were stained with FITC-conjugated PNA and PE-conjugated goat anti–mouse B220. Cells were analyzed on an LSRII and the populations of B220$^+$PNA$^+$ and B220$^+$PNA$^-$ were calculated by FlowJo software. Closed circles, WT BALB/c; open circles, Fcγ$^{-/-}$ mice. Each circle represents an individual mouse and the horizontal bar denotes the mean. *, P ≤ 0.05. (d) AID induction in germinal center B cells. Both WT and Fcγ$^{-/-}$ mice were immunized at day 0 and killed at day 12. Purified B cells were further stained with FITC-conjugated PNA. B220$^+$ and PNA$^+$ cells were sorted as germinal center cells and B220$^+$PNA$^-$ cells were sorted as nongerminal center cells. Total RNA was extracted from each population and AID expression was measured by real-time PCR. The analysis was performed on B cells isolated from each of three WT or Fcγ$^{-/-}$ mice. Mean ± SD.of the individual mice is shown. *, P ≤ 0.05.

have shown that DCs can induce naive B cells to proliferate in an IL-12–dependent manner. We therefore examined whether BM-derived DCs (BMDCs) from Fcγ^{-/-} mice were more potent producers of IL-12 and stimulators of B cell proliferation. IL-12 was measured in immature and LPS-matured BMDCs by intracellular flow cytometry and cytokine ELISA. Flow cytometry, which measured IL-12 p40, demonstrated a twofold increase in the number of DCs producing IL-12 in Fcγ^{-/-} mice (Fig. 6 a). A cytokine ELISA for IL-12 p40/70 detected IL-12 production only by LPS-stimulated BMDCs and confirmed a two- to threefold increase in production by Fcγ^{-/-} DCs (Fig. 6 b). Real-time PCR also demonstrated increased induction of IL-12p35 and p40 in LPS-stimulated BMDC from Fcγ^{-/-} mice (Fig. 6 c). Fcγ^{-/-} BMDCs also displayed significantly higher expression of MHC II, CD80, and CD86 than WT BMDCs (Fig. S2, available at http://www.jem.org/cgi/content/full/jem.20070731/DC1). Finally, we measured IL-12 expression in splenic DCs after MAP peptide immunization in vivo. Both WT and Fcγ^{-/-} mice were immunized. On days 1 and 3, total splenic DCs were purified and further cultured for 16 h to permit cytokine secretion. Fig. 6 d demonstrates that splenic DCs from Fcγ^{-/-} mice expressed about twofold more IL-12 than DCs from WT mice by day 3.

Because there are other cell types that can produce IL-12 upon activation, we measured production of IL-12 by macrophages and B cells. As seen in previous studies, LPS stimulation strongly induced production of IL-12 from peritoneal macrophages, but there was no difference between WT and Fcγ^{-/-} macrophages. B cells from WT and Fcγ^{-/-} mice also produced equal amounts of IL-12 p40 after upon LPS and LPS plus anti-CD40 antibody stimulation. (Fig. 6 e).

To confirm that the increased IL-12 could lead to an expanded B cell population, naive WT B cells were cultured with anti-CD40 antibody and irradiated BMDCs from either Fcγ^{-/-} or WT mice. After 5 d in culture, B cells proliferated in the presence of Fcγ^{-/-} BMDCs, whereas little or no BMDC-dependent proliferation was seen in the presence of WT BMDCs (Fig. 7 a). Furthermore, when a neutralizing anti–IL-12 antibody was added at the beginning of the culture, B cell proliferation driven by Fcγ^{-/-} BMDCs decreased by as much as 80% (Fig. 7 b). Because anti–IL-12 antibody recognizes both the p35 and the p40 subunits of IL-12 and p40 is also a subunit of IL-23, there is a possibility of inhibition of both cytokines by the anti–IL-12 antibody. To address this problem, IL-12a (p35)–specific siRNA was used. Transfection efficiency was determined and specificity of IL-12a siRNA was confirmed using control siRNA and analyzing gene expression of IL-12b (Fig. S3, available at http://www.jem.org/cgi/content/full/jem.20070731/DC1). Consistent with the results using anti–IL-12 antibody, IL-12a siRNA transfection of BMDCs abrogated the proliferation of B cells (Fig. 7 c). The inhibition was specific, as transfection with control siRNA showed no significant reduction in B cell proliferation. Therefore, Fcγ^{-/-} DCs are potent stimulators of B cell proliferation, and their stimulatory function depends largely on the production of IL-12.
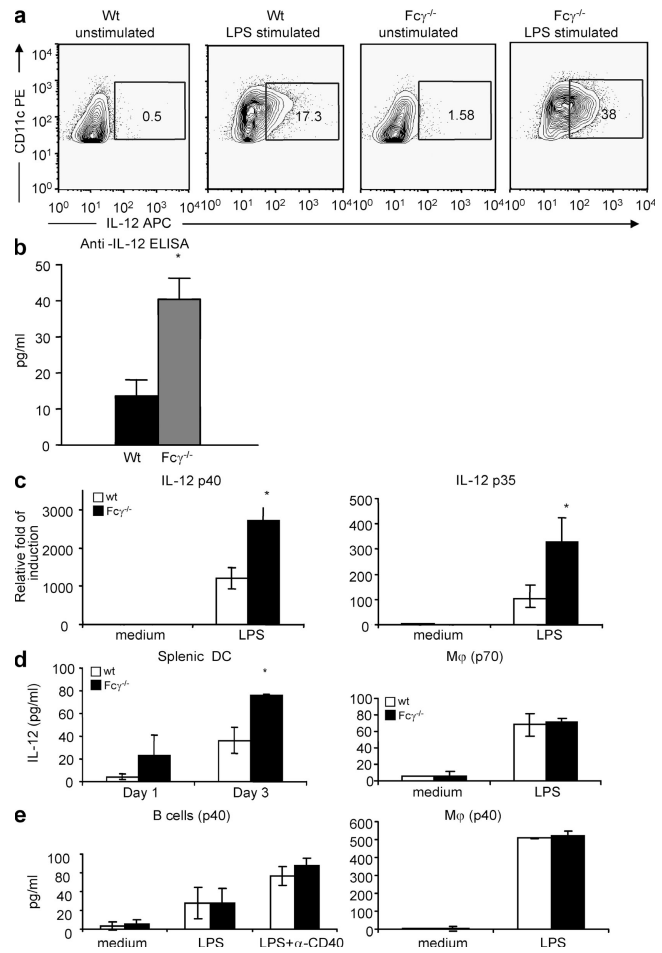

Figure 6. Fcγ^{-/-} BMDCs exhibit increased IL-12 secretion compared with WT BMDCs. (a) Unstimulated and LPS-stimulated BMDCs were stained with anti-CD11c PE extracellularly and anti–IL-12-APC intracellularly and analyzed by flow cytometry. These results are representative of three independent experiments. (b) LPS-stimulated BMDCs were cultured for 24 h, and an anti–IL-12 cytokine ELISA was performed on the supernatant. Fcγ^{-/-} BMDCs are shown in gray and WT BMDCs are shown in black. IL-12 levels were not detectable by ELISA in unstimulated cultures. The assay was performed in triplicate. *, $P \leq 0.05$. Results are representative of mean $\pm$ SD of three independent experiments. (c) Total RNA was purified from unstimulated or LPS-stimulated BMDCs for 4 h. 1 μg of total RNA was used for PCR. S18 rRNA gene was amplified as an internal control. Relative expression of IL-12a and b was calculated as described in Materials and methods. *, $P \leq 0.05$. The results are mean $\pm$ SD of three experiments. (d) IL-12 produced by splenic DCs. Mice were immunized as described previously and splenic DCs were purified on days 1 and 3 after immunization. Cells were plated at 10^6 /ml in 24-well plates for 16 h. IL-12 in the supernatant was analyzed by ELISA. *, $P \leq 0.05$ (mean $\pm$ SD of three individual mice). (e) Splenic B cells and peritoneal macrophages were isolated and the purity of the populations was determined as described in Materials and methods. For B cells, 10^6 cells/ml were plated in 24-well plates alone, with 5 μg/ml of LPS, or with 5 μg/ml LPS with 20 μg/ml of activating anti-CD40 antibodies and incubated for 18 h. Supernatants were harvested and IL-12 p40 was measured as described. For macrophages, 10^6 cells/ml were cultured in 24-well plates with or without 2 μg/ml LPS for 18 h. IL-12 p40 and p70 in the supernatant was measured by ELISA (mean $\pm$ SD of four individual mice).

IL-12 secretion influences the differentiation of plasma cells in vivo

To confirm that the increased IL-12 production by DCs accounted for the altered antibody response seen in vivo in Fcγ$^{-/-}$ mice, we determined if WT mice given supplemental IL-12 would produce more plasma cells in spleen. WT mice were injected i.p. with 1 µg of either soluble IL-12 or saline on days −1, 0, and +1 of the immunization schedule. Antigen boosts were given with no additional IL-12. 11 d after the last boost, WT mice treated with IL-12 had approximately three-fold more splenic antibody-secreting cells than untreated mice, which is similar to the difference observed in Fcγ$^{-/-}$ mice (Fig. 8 a). IL-12–treated WT mice also experienced an ∼35% decrease in BM plasma cells, which is also similar to Fcγ$^{-/-}$ mice (Fig. 8 b). Thus, exogenous IL-12 caused WT mice to acquire a phenotype of antigen-specific B cells similar to that of Fcγ$^{-/-}$ mice. We confirmed this observation in a study of
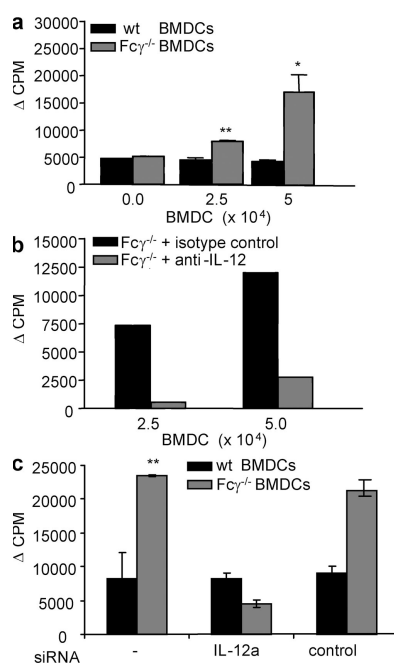
Fcγ$^{-/-}$.IL-12a$^{+/-}$ mice. First, we examined the effect of IL-12 in WT, Fcγ$^{-/-}$ mice, or Fcγ$^{-/-}$.IL-12a$^{+/-}$ mice. The level of expression of IL-12 p35 assessed by real-time PCR showed decreases in both WT and Fcγ$^{-/-}$.IL-12a$^{+/-}$ mice compared with Fcγ$^{-/-}$ mice (Fig. S4, available at http://www.jem.org/cgi/content/full/jem.20070731/DC1). MAP peptide–immunized Fcγ$^{-/-}$.IL-12a$^{+/-}$ mice generated a low number of anti-peptide antibody secreting cells in spleen, which is similar to WT mice (Fig. 8 c), and a high number of plasma cells in the BM, which is also similar to WT mice (Fig. 8 d). The enhanced B cell response of the Fcγ$^{-/-}$ mice can, therefore, be attributed, at least in part, to increased IL-12 production by DCs, as it is altered when IL-12 production is diminished.

DISCUSSION

Understanding mechanisms underlying the commitment to a particular B cell fate has clinical importance. Memory cells can proliferate extensively upon secondary challenge, and long-lived plasma cells can secrete antibody for long periods of time without antigen contact. Therefore, the prevalence of autoreactivity in the memory population may result in a chronic antibody-mediated disease. In contrast, short-lived plasma cells may generate large amounts of a pathogenic
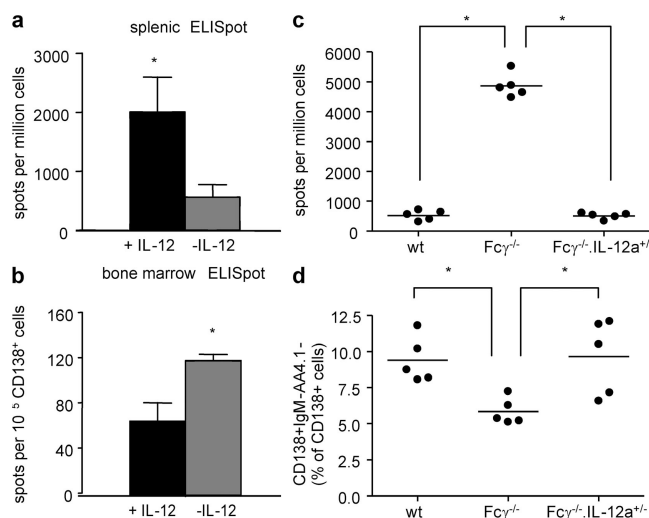

Figure 7. Lymphocyte proliferation with BMDCs. (a) 5 × 10^4 WT B cells were cultured for 6 d in the presence of anti-CD40 mAb with varying numbers of irradiated BMDCs from either WT (black bars) or Fcγ$^{-/-}$ (gray bars) mice. B cell proliferation was determined by ^{3}H incorporation. The assay was performed in triplicate. *, P ≤ 0.05; **, P ≤ 0.01. These results are mean ± SD of three independent experiments. (b) The proliferation assay was performed as above with WT B cells and Fcγ$^{-/-}$ BMDCs in the presence (gray bars) or absence (black bars) of 10 µg of neutralizing monoclonal anti–IL-12 antibody. The results are reported as the difference in proliferation between cultures in which BMDCs are present and absent. These results are mean ± SD of three independent experiments. (c) A proliferation assay was performed with siRNA-transfected BMDCs. BMDCs were generated from WT mice and Fcγ$^{-/-}$ mice. 10 µM of either anti–IL-12a or control siRNA was transfected, as described in Materials and methods, at day 7 of culture. The next day, siRNA-transfected and -untransfected DCs were incubated with 1 µg/ml LPS to mature DCs. Proliferation assays were performed as described in Materials and methods. The results are mean ± SD of five indivual mice.

Figure 8. IL-12 treatment of WT mice mimics the plasma cell phenotype observed in Fcγ$^{-/-}$ mice. BALB/c WT mice were injected i.p. with 1 µg rIL-12 (black bars) or saline (gray bars) on days −1, 0, and 1 after immunization with MAP peptide. Mice were boosted as previously described. (a) Splenocytes were taken on day 25 after immunization, and peptide-specific ELISPOTs were performed. n = 5 mice in each group. (b) BM was taken on day 25 after primary immunization, and CD138$^+$ cells were sorted to perform antipeptide ELISPOT assays. The number of spots was counted and enumerated as in the figure. *, P ≤ 0.05. WT, Fcγ$^{-/-}$, or Fcγ$^{-/-}$.IL-12a$^{+/-}$ mice were immunized with 100 µg MAP peptide. (c) Splenocytes were taken on day 25 after primary immunization. Peptide-specific ELISPOTs were performed, and spots were enumerated. Each dots represent individual mice. *, P ≤ 0.05. (d) BM was taken on day 25 after immunization. CD138$^+$IgM$^-$AA4.1$^-$ plasma cells were enumerated as a percentage of CD138$^+$ cell. *, P ≤ 0.05.

antibody that, as shown in this study, does not necessarily need to be of the highest affinity to cause organ damage.

Through the analysis of Fcγ$^{-/-}$ mice, we have demonstrated that DCs participate in determining B cell differentiation in vivo. Fcγ$^{-/-}$ B cells became predominantly splenic plasma cells upon activation instead of forming the more heterogeneous population of short-lived and long-lived plasma cells and memory cells seen in WT mice. Current data suggest that the majority of splenic plasma cells are short lived, whereas plasma cells in the BM can be either short lived or long lived (15, 18, 19, 24). In our study, Fcγ$^{-/-}$ mice had a transient surge of plasma cells in the spleen, while displaying a diminished rise in plasma cells in the BM and a reduced memory B cell response. In contrast, WT mice had a smaller population of splenic plasma cells and an increase in BM plasma cells after immunization and demonstrated B cell memory upon secondary challenge with antigen. Fcγ$^{-/-}$ mice produced significantly higher serum titers of specific antibody than WT mice and displayed class switching to IgG2a as well as IgG1. The increase in serum antipeptide and anti-DNA response appears to be an FcR-dependent phenomenon because FcγRI$^{-/-}$ immunized with MAP peptide showed a similar phenotype (Fig. S5, available at http://www.jem.org/cgi/content/full/jem.20070731/DC1). These features of the response may account for the increased glomerular dysfunction. Interestingly, antibodies from Fcγ$^{-/-}$ displayed less affinity maturation. This serologic data were confirmed by the demonstration of reduced GL-7–positive cells in splenic B cells of Fcγ$^{-/-}$ mice (unpublished data) and less somatic mutation in antigen-specific hybridomas. Because some studies suggest that short-lived and long-lived plasma cells arise from completely separate precursors (25), we are currently studying the B cells responding to antigen in WT and Fcγ$^{-/-}$ mice to determine if the same clones are activated or whether the plasma cell precursors differ between the strains.

DCs have previously been shown to mediate a critical function in B cell activation by transporting antigen from the periphery to T and B cells (26). The altered B cell phenotype we observed in Fcγ$^{-/-}$ could also be traced to the influence of Fcγ$^{-/-}$ DCs and IL-12. Fcγ$^{-/-}$ DCs had a more mature phenotype and produced at least twofold more IL-12 than WT DCs. Several studies have established a role for IL-12 in B cell differentiation and function. IL-12 can induce plasma cell formation and B cell heavy chain class switching to IgG1 and IgG2a. The switch to IgG2 is IFN-γ–dependent, whereas the promotion of differentiation to plasma cells and the switch to IgG1 does not require IFN-γ (27). Studies in human primary B cells have also shown that IL-12 up-regulates IL-12Rβ2 expression and IFN-γ production by B cells, possibly allowing them to function as B effector cells and promote the activation of Th1 cells (28). Notably, although IL-12 promotes short-lived plasma cells, perhaps in synergy with CD40L (27), memory B cell differentiation occurs independently of IL-12 (22, 23). In our study, when IL-12 was administered to WT mice, the mice responded to antigen immunization with the generation of more splenic plasma cells and fewer BM

plasma cells, a pattern mimicking that seen in immunized Fcγ$^{-/-}$ mice. Therefore, IL-12 produced by DCs seems to be highly influential in directing B cell differentiation. It is possible that this difference in differentiation pathway reflects a change in the environment in which the B cell resides rather than a direct effect on the B cell. We do not favor this explanation, as chemokine expression in the spleen is similar in both strains (Fig. S6, available at http://www.jem.org/cgi/content/full/jem.20070731/DC1). Furthermore, IL-12 has been shown by others to act directly on B cells (21). Interestingly, CR2 (CD21/CD35) has also been reported to diminish the development of long-lived plasma cells while leaving intact the generation of short-lived plasmablasts, germinal center, and memory B cells. This effect is mediated through the regulation of Blimp-1 and XBP-1, which are critical transcription factors in plasma cell differentiation (29). CR2, like FcR, appears to function through a B cell–intrinsic pathway that specifically arrests the differentiation of long-lived plasma cells. We should note, however, that antigen-specific T cell proliferation was enhanced in Fcγ$^{-/-}$ mice. The enhanced number of antigen-specific T cells expressing CD40L and available to interact with antigen-specific B cells may also contribute to the preferential generation of short-lived plasma cells. Thus, both the direct action of DCs on B cells as well as the action of T cells in Fcγ$^{-/-}$ mice may contribute to skewing the B cell response.

Although the differences in IL-12 production between the mouse strains may seem small, we have previously shown in studies of hormonal effects on B cells that a 20% change in expression of CD22 can affect B cell receptor signaling and alter negative selection (30). Recently, McGaha et al. (31) have shown that a 50% increase in FcγRIIb expression in B cells can prevent disease in lupus-prone mice. Thus, it should not be surprising that a twofold increase in IL-12 production by DCs can affect B cell differentiation. In fact, a study of experimental myasthenia gravis in mice also demonstrated that exogenous IL-12 given in a similar protocol led to increased serum antibody (27).

A previous study reported no alteration in humoral response to the hapten NP in Fcγ$^{-/-}$ mice. This study was performed on C57BL/6 mice deficient in the FcR γ chain and may reveal a strain-dependent difference in FcR γ chain function. It is also possible, however, that the force of selection for high-affinity antibodies in the NP model is so strong that differences in B cell differentiation were obscured. Some effects were seen that were similar to those we report. For example, in the reported study that Fcγ$^{-/-}$ mice had fewer splenic germinal centers after immunization.

We do not yet fully understand why the absence of the γ chain leads to the observed DC phenotype. Studies on γ chain–deficient mice have focused on alterations in expression and function of FcRI, FcRIII, and FcRIV (32). To confirm that the serological changes were mediated through FcR engagement, we have immunized FcRIII-deficient mice with MAP peptide. These mice show increased serum antipeptide antibodies (fivefold increase) and an activated phenotype of BMDCs. Similarly, DCs derived from BM cells under

serum–free conditions also display an activated phenotype, which is, again, consistent with FcR engagement modulating DC function (26). The activated phenotype was abrogated by addition of purified IgG to the culture. Although γ chain–containing Fc receptors have been demonstrated to be activating receptors, we speculated that engagement of these receptors may diminish the response to other activating receptors. Such reciprocal regulation of toll-like receptor 9 and IgE receptor signaling has already been demonstrated. Production of type I IFN by plasmacytoid DC is inhibited by preexposure of FcεRI to IgG (33). These two signaling pathways counterregulate the development of Th1 and Th2 immune response. Park-Min et al. (34) recently demonstrated that immune complexes binding to FcγRIII suppresses LPS-mediated IFNγ signaling in both human peripheral blood mononuclear cells derived macrophages and murine peritoneal macrophages. A recent publication reported that human peripheral monocyte-derived DC cultures exposed to immune complexes show diminished differentiation. Furthermore, in response to TLR-mediated stimulation, they produced less IL-12 (35). This inhibition was mediated mainly through FcγRI but, to a lesser extent by FcγRII. Thus, there is precedent for an absence of engagement of activating FcRs permitting an enhanced response in other activation pathways. Although the mechanism for the altered function of Fcγ$^{-/-}$ DC requires further confirmation, it is apparent that the difference in IL-12 production by DCs affects B cell differentiation. This study reports the first in vivo manipulation that leads to differential formation of short-lived and long-lived plasma cells. Understanding how to modulate B cell differentiation will facilitate an appreciation of the role of both short-lived and long lived plasma cells. Furthermore, knowledge of the B cell phenotype responsible for the production of antiself or antimicrobial antibodies will help in the design of therapeutic strategies in autoimmune disease, as well as in optimizing vaccine development.

MATERIALS AND METHODS

Mice. 5–10-wk-old female Fcγ$^{-/-}$ mice (Fcer1g(BALB/cBy)) on the BALB/c background and WT BALB/c mice were purchased from Taconics. The mice were housed in a specific pathogen-free barrier facility. IL-12a$^{-/-}$ mice (C.129S1(B6)-*Il12a^{tm1Jm}*/J) were purchased from Jackson ImmunoResearch Laboratories. IL-12a$^{-/-}$ mice were bred to Fcγ$^{-/-}$ mice for the generation of mice that were IL-12 p35$^{+/-}$ and Fcγ$^{-/-}$. These studies were approved by the Institutional Animal Care and Use Committees of the Albert Einstein College of Medicine, Columbia University Medical Center, and Feinstein Institute for Medical Research.

Antigens. The peptides DWEYSVWLSN, linked to an eight-branched poly-lysine backbone (MAP peptide), and ADGSGGRDEMQASMWS were purchased from both Invitrogen and AnaSpec, Inc. The peptide ADGSGGRDEMQASMWS (10–2) was conjugated to BSA with glutaraldehyde as previously described (12).

Immunizations. Mice were immunized i.p. with 100 µg MAP peptide or ADGSGGRDEMQASMWS-BSA in CFA (Becton Dickinson) on day 0 and then boosted in IFA (Becton Dickinson) on days 7 and 14. For the recall assay, mice were immunized i.p. with 100 µg MAP peptide in CFA on day 0 and boosted with antigen in IFA on day 56.

Adoptive transfer of B cells to muMT mice. 6-8-wk-old WT and Fcγ$^{-/-}$ mice were killed and total splenic B cells were purified. Recipient µMT mice were injected with 2×10^7 cells intravenously. 2 wk after transfer, both WT B cell–reconstituted and Fcγ$^{-/-}$ B cell–reconstituted muMT mice were immunized with MAP peptide as described. The antipeptide response from both groups was measured every 2 wk until 6 wk after immunization.

ELISAs. EIA/RIA high binding 96-well plates (Costar; Corning) were coated with 15 µg/ml of the relevant peptide. For dsDNA ELISAs, plates were coated with 100 µg/ml of sonicated calf thymus DNA (Sigma-Aldrich) that was filtered through a 0.45-µm of nitrocellulose Millex–HA syringe filter (Millipore) to produce dsDNA. Plates were then blocked with 3% FCS or 5% milk. Alkaline phosphatase–conjugated anti–mouse total IgG or anti–mouse isotype-specific antibodies (SouthernBiotech) were used as secondary antibodies, and plates were developed with *p*-nitrophenyl phosphate (Sigma-Aldrich). OD was monitored at 405 nm.

ELISAs determining the apparent affinity of peptide-specific antibodies were performed with the following modification: sera were preincubated with varying concentrations of the relevant peptide before being loaded onto the antigen-coated plates. The K_a was calculated as the reciprocal of the molar concentration of peptide inhibiting 50% of the binding (10).

Memory response. WT and Fcγ$^{-/-}$ mice were immunized and boosted as described above. Mice were bled every 2 wk to measure the antipeptide response in serum. After 8 wk, mice were challenged with 100 µg MAP peptide in IFA, and blood was drawn 5 d later to analyze the antipeptide antibody response.

Immunohistochemistry of kidneys. To determine glomerular IgG deposition, kidneys were obtained 13 wk after the initial immunization, fixed in 10% paraformaldehyde, and embedded in paraffin. Sections were blocked with 2% BSA and stained with biotinylated goat anti–mouse IgG. Alkaline phosphatase–labeled ABC reagent from the VECTASTAIN ABC kit (Vector Laboratories) was added. Sections were developed with 5-bromo-4-chloro-3-indolyl phosphate-toluidine salt and nitroblue tetrazolium chloride substrate (Invitrogen). Proteinuria was determined by color comparison using Multistix (Sigma-Aldrich).

Purification of B cells. For B cell purification, single-cell suspensions were prepared from splenocytes. After red blood cell lysis, cells were incubated with biotinylated anti-CD3, anti-CD11b, and anti-CD11c mAb (BD Biosciences), and B cells were isolated by negative selection with magnetic streptavidin-linked Dynabeads (Invitrogen). After depletion, >90% of the remaining cells were B220$^+$ by flow cytometry. All flow cytometry was performed on a FACSCalibur (Becton Dickinson) and analyzed with FlowJo Software (Tree Star, Inc.).

Purification of T cells. Mice were immunized in the right front and hind footpads with 100 µg MAP peptide in 100 µl of 1:1 PBS/CFA and in the left front and hind footpads with 100 µl of 1:1 PBS/CFA alone (50 µl/footpad). 1 wk later, left and right popliteal, axillary, and brachial lymph nodes were harvested, and a single cell suspension was prepared. Red blood cells were lysed, and cells at 2×10^7 cells/ml were incubated at 4°C for 30 min with supernatants from the following ATCC cell lines: TIB-120 (anti-A^{b,d,q} and anti-E^{d,k}), HB-198 (anti-F4/80), and anti-B220 (BD Biosciences). Excess antibody was washed away and the cells were incubated with sheep anti–rat IgG Dynal/Dynal beads at 4°C for 30 min. T cells were isolated by magnetic bead depletion (Invitrogen) and were demonstrated by flow cytometry to be >95% pure.

Peritoneal macrophages. To collect peritoneal macrophages, WT and Fcγ$^{-/-}$ mice were injected with 2 ml of 3% aged thioglycollate i.p. On day 4, mice were killed and macrophages were harvested in Hank's balanced salt solution. The purity of the cell population was assessed by staining with F480 antibody. All samples were >85% F480 positive.

Purification of DCs. BMDCs were generated according to a previously described protocol (36). In brief, BM was harvested and red blood cells were lysed. T cells and B cells were depleted by incubating the cells with the ATCC supernatants TIB-120, TIB-211 (anti-CD8), TIB 207 (anti-CD4), and TIB-146 (anti-B220) in the presence of rabbit complement (Pel-Freez Biologicals). The remaining cells were cultured in RPMI 1640 with 5% FCS and GM-CSF–containing supernatant from J558L cells (gift of the laboratory of R. Steinman, The Rockefeller University, New York, NY). Cells were given fresh medium on days 2 and 4. On day 6, the nonadherent cells were collected and were incubated overnight in medium with or without 50 ng/ml LPS from *Escherichia coli* serotype 055:B5 (Sigma-Aldrich). To further deplete monocytes, the cells were plated for 2 h, and nonadherent cells were collected. The depleted cells were >85% CD11c$^+$ by flow cytometry.

To purify splenic DCs, a modification of the original method of Steinman et al. (37) was used. In brief, spleen cell suspensions were prepared by digestion with 400 U/ml collagenase D at 37°C for 25 min, followed by 0.5 M EDTA. Total splenocytes were washed and resuspended in 30% BSA. Ice-cold PBS was loaded on top of the mixture. DCs were collected from the interface after centrifugation at 2,200 rpm for 30 min. To increase the purity of DCs, we used negative selection methods with a mouse DC enrichment set (BD Biosciences). After two steps of purification, the purity was measured by flow cytometry and ∼75–80% of cells were CD11c$^+$.

Enumeration of plasma cells. Antigen-specific plasma cells were enumerated in the spleen and BM of femurs by performing peptide-specific ELISPOT assays. For plasma cells in the spleen, MAP peptide–immunized mice were killed and splenocytes were harvested. Red blood cells were lysed, and the splenocytes were added to plates coated with 10 μg/ml MAP peptide and blocked with 10% FCS. The plates were centrifuged at 1,000 rpm for 5 min and incubated overnight at 37°C. The next day, splenocytes were washed stringently and biotinylated goat anti–mouse IgG (Southern-Biotech) was added for 2 h at 37°C. Washed plates were incubated with streptavidin-alkaline phosphatase (SouthernBiotech) for 2 h and developed with 5-bromo-4-chloro-3-indolyl phosphate *p*-toluidine salt (Sigma-Aldrich). Spots were counted manually using a dissecting microscope. To enumerate plasma cells in the BM, CD138$^+$ cells were identified by flow cytometry, and CD138$^+$ cells from WT and Fcγ$^{-/-}$ mice were sorted on a FACSAria and plated for MAP peptide–specific ELISPOT analysis.

Spleen histology. Spleens were harvested on days 0, 4, 8, 12, and 16 after immunization and snap frozen in Tissue-Tek O.C.T. compound (Sakura Finetek). Sections were incubated with anti–mouse B220-FITC and CD138-PE, or B220-PE and PNA-FITC, and were visualized using a fluorescent microscope (AxioCam II; Carl Zeiss, Inc.).

AID expression in germinal center B cells. Expression of AID gene was measured in purified germinal center B cells. WT and Fcγ$^{-/-}$ mice were immunized with 100 μg of MAP peptide in CFA on day 0. On day 10, mice were killed and splenic B cells were purified by depletion of non-B cells: splenocytes were incubated with biotinylated anti-CD43, anti-CD11c, and anti-CD90.2 (BD Biosciences) and bound cells were removed by streptavidin-conjugated magnetic beads. B220 and PNA double-positive cells were isolated on a FACSAria as germinal center B cells, and B220-positive and PNA-negative fractions were collected as control cells. AID expression was measured by real-time PCR using total RNA from each fraction. Gene-specific primers for AID were purchased from TaqMan, and real-time PCR was performed as described in Materials and methods.

Analysis of DC phenotype and cytokine secretion. For cytokine secretion, intracellular flow cytometry was performed. LPS-treated or untreated BMDCs were cultured at 5×10^5/ml with 10 μg/ml brefeldin A (Sigma-Aldrich) for 5 h. The cells were then stained with anti-CD11c PE (BD Biosciences) and fixed in 2% paraformaldehyde for 10 min before staining with anti–IL-12 APC or anti–IL-10 APC in 0.3% saponin for 30 min. For cytokine analysis by ELISA, 10^6 BMDCs were cultured for an additional 24 h af-

ter LPS treatment, and cytokines were assayed in the culture supernatant using anti–mouse cytokine ELISA kits. Cytokine concentrations were determined based on standard curves.

For real-time PCR, total RNA was prepared from BMDCs either unstimulated or LPS-stimulated for 4 h using TRIzol Reagent (Invitrogen). 1 μg DNA-free RNA was reverse transcribed to cDNA using SuperScript III First-Strand Synthesis system for RT-PCR (Invitrogen). Real-time PCR was performed with TaqMan Universal PCR Master Mix (Applied Biosystem) on an iCycler iQ instrument (Bio-Rad Laboratories). Amplification conditions were 50°C for 2 min and 95°C for 10 min, followed by 40 cycles of 95°C for 15 s and 60°C for 1 min. Primers for 18s ribosomal RNA, IL-12a, IL-12b, and AID were purchased from Applied Biosystems. Relative expression was determined using the following formula: relative expression = $2^{-(\Delta\Delta CT)}$, where $\Delta\Delta CT$ = [Ct (gene of interest sample) - Ct(18s rRNA sample)] - [Ct(gene of interest calibrator) - Ct(18s rRNA calibrator)]. (See the $\Delta\Delta$ CT methods, Taqman Bulletin 2; Applied Biosystems). Data are presented as the mean ± SD of three experiments.

In vivo cytokine production by splenic DCs. BALB/c WT or Fcγ$^{-/-}$ mice were immunized with 100 μg MAP peptide in CFA i.p. Each group of mice was killed on either day 1 or 3 after immunization. Splenic DCs were purified as described in Materials and methods and cultured in RPMI 1640 supplemented with 10% FCS for 16 h. Supernatant was collected and cytokine production was analyzed by ELISA.

BMDC and B cell coculture assays. BMDCs were stained with anti-CD11c PE (BD Biosciences) and sorted on a MoFlo Cell Sorter (Dako). More than 95% of the sorted cells were CD11c$^+$. Mature BMDCs, irradiated with 1,500 rads, were cultured with 5×10^4 B cells in triplicate in RPMI with 10% FCS in the presence of 20 μg/ml of purified anti-CD40 antibody (BD Biosciences). In some assays, 10 μg/ml of purified anti–IL-12 antibody (BD Biosciences) was added to the culture. 5 d later, 1 μCi of ^{3}H-thymidine was added to each well for 8 h, and the incorporated radioactivity was determined. To block the secretion of IL-12 during the coculture, siRNA (siRNA ID#: 102773l; Ambion) targeting the IL-12a gene was transfected to BMDC according to the manufacturer's protocol. In brief, irradiated BMDCs cultured from both WT and Fcγ$^{-/-}$ mice were transfected with 1 and 10 μM of anti–IL-12a specific or negative control siRNA by siPORT NeoFX (Ambion). The next day, siRNA/transfection agents were removed and 5×10^4 splenic B cells were added to the culture.

T cell proliferation. T cells were purified from lymph nodes of MAP peptide–primed WT or Fcγ$^{-/-}$ mice as described in Materials and methods. BMDCs were prepared from nonimmunized WT and Fcγ$^{-/-}$ mice and pulsed with MAP peptide on day 6 of culture. On day 7, $1–3 \times 10^5$ primed T cells were cocultured in triplicate for 72 h with 5×10^4 irradiated DCs. Cells were pulsed with 0.5 μCi of ^{3}H-thymidine for the last 8 h. Cells were harvested, and the incorporated radioactivity was counted.

Analysis of Vβ usage and cytokine ELISAs. Cells from the draining lymph nodes of naive mice or mice immunized 7 d earlier with MAP peptide in CFA or CFA alone were harvested and plated at 3×10^6 cells/ml in IMDM supplemented with 10% FCS, 2 mM glutamine, 100 U/ml penicillin, 100 μg/ml streptomycin, and 50 μM β-mercaptoethanol in the presence of 50 μg/ml MAP peptide. 7 d later, the cultures were supplemented with 50 U/ml of recombinant human IL-2 (Invitrogen) and 3×10^6 RBC-depleted irradiated (1,500 rads) splenocytes/ml along with fresh medium. 14 d after the initial culture, cells were collected. 2×10^5 cells were stained with 100 μl of 1 μg/ml CD4-PE in 2% FCS/PBS for 30 min on ice and then stained for the various Vβ chains using FITC-labeled antibodies. All labeled antibodies were obtained from BD Biosciences and data were acquired using a FACScan (Becton Dickinson). Peptide-specific T cells were identified by comparison of lymph node cultures from mice immunized with MAP peptide in CFA to those from mice immunized with CFA alone. Little proliferation was detected in the latter with 3–4 times as many live cells found in the peptide-specific cultures compared with the CFA controls.

Cytokine ELISAs were performed on purified lymph node T cells for the detection of IL-2 and IFN-γ. After 72 h of culture, T cell supernatants were tested using the mouse cytokine ELISA kit (Endogen). Cytokine concentrations were determined based on a standard curve.

In vivo IL-12 treatment. Mice were injected i.p. with 1 μg rIL-12 or saline on days −1, 0, and 1 after immunization with MAP peptide in CFA. Mice were then boosted as described in Materials and methods with no further administration of IL-12. On day 25, mice were killed, and a peptide-specific ELISPOT assay was performed on splenocytes. BM cells were harvested, and plasma cells were enumerated by flow cytometry as described above.

Generation of hybridomas and sequencing J_H2-J_H4 region. BALB/c WT and Fcγ$^{-/-}$ mice were immunized as described in Materials and methods. 3 d after boosting, mice were killed and total splenocytes were harvested. Cells were fused with the NSO myeloma fusion partner using standard hybridoma technology. 2 wk after fusion, antipeptide antibody secreting clones were screened. Genomic DNA was purified from positive clones by TRIzol reagent. The J_H2–J_H4 region was amplified using Pfu turbo (Stratagene) followed by previously described protocol (38). PCR was performed with the following primers: 5′ primer, 5′-GGCACCACTCTCACAGTCTCCT-CAGG-3′; and 3′ primer, 5′-TGAGACCGAGGCTAGATGCC-3′. PCR conditions were the following: 95°C for 30 s, 60°C for 30 s, and 72°C for 15 min for 35 cycles. PCR products were purified and sequenced at the DNA sequencing facility at the Columbia University Medical Center.

In vivo depletion of CD4+ T cells. The GK1.5 monoclonal antibody (rat IgG2b anti–murine CD4) was used for in vivo depletion of CD4 T cells. 500 μg of antibody was administered by i.p. injection of 0.1 ml of saline on days −1, 0, and 1 after immunization with MAP peptide in CFA. Blood samples were collected on day 0 and every 2 wk for 8 wk.

Statistics. Comparisons between groups were performed by Student's t test. A two-way analysis of variance test was used to compare curves in ELISA assays. Error bars represent SD values, and p-values <0.05 were considered to be statistically significant.

Online supplemental material. Fig. S1 shows serum anti–MAP peptide IgM titer. Fig. S2 shows the increased surface activation markers in BMDCs by FACS analysis. Fig. S3 shows the specific inhibition of IL-12a expression after siRNA treatment in BMDCs. Fig. S4 shows the relative expression of IL-12a in splenic DCs from WT, Fcγ$^{-/-}$, and Fcγ$^{-/-}$.IL-12a$^{+/-}$ mice. Fig. S5 shows titer of anti–MAP peptide and anti-dsDNA antibody in serum from WT, Fcγ$^{-/-}$, and FcRI$^{-/-}$ mice. Fig. S6 is for the expression of chemokine/chemokine receptor in splenic B cells and DCs. Table S1 shows the number of germinal centers in MAP peptide–immunized WT and Fcγ$^{-/-}$. Online supplemental material is available at http://www.jem.org/cgi/content/full/jem.20070731/DC1.

REFERENCES

1. Putterman, C., and B. Diamond. 1998. Immunization with a peptide surrogate for double-stranded DNA (dsDNA) induces autoantibody production and renal immunoglobulin deposition. *J. Exp. Med.* 188:29–38.

2. Khalil, M., K. Inaba, R. Steinman, J. Ravetch, and B. Diamond. 2001. T cell studies in a peptide-induced model of systemic lupus erythematosus. *J. Immunol.* 166:1667–1674.

3. Takai, T., M. Li, D. Sylvestre, R. Clynes, and J.V. Ravetch. 1994. FcR gamma chain deletion results in pleiotrophic effector cell defects. *Cell.* 76:519–529.

4. Clynes, R., C. Dumitru, and J.V. Ravetch. 1998. Uncoupling of immune complex formation and kidney damage in autoimmune glomerulonephritis. *Science.* 279:1052–1054.

5. Benson, M.J., L.D. Erickson, M.W. Gleeson, and R.J. Noelle. 2007. Affinity of antigen encounter and other early B-cell signals determine B-cell fate. *Curr. Opin. Immunol.* 19:275–280.

6. Shapiro-Shelef, M., K.I. Lin, L.J. McHeyzer-Williams, J. Liao, M.G. McHeyzer-Williams, and K. Calame. 2003. Blimp-1 is required for the formation of immunoglobulin secreting plasma cells and pre-plasma memory B cells. *Immunity.* 19:607–620.

7. Chacko, G.W., S. Tridandapani, J.E. Damen, L. Liu, G. Krystal, and K.M. Coggeshall. 1996. Negative signaling in B lymphocytes induces tyrosine phosphorylation of the 145-kDa inositol polyphosphate 5-phosphatase, SHIP. *J. Immunol.* 157:2234–2238.

8. Cyster, J.G., and C.C. Goodnow. 1995. Protein tyrosine phosphatase 1C negatively regulates antigen receptor signaling in B lymphocytes and determines thresholds for negative selection. *Immunity.* 2:13–24.

9. Otipoby, K.L., K.E. Draves, and E.A. Clark. 2001. CD22 regulates B cell receptor–mediated signals via two domains that independently recruit Grb2 and SHP-1. *J. Biol. Chem.* 276:44315–44322.

10. Nieto, A., A. Gaya, M. Jansa, C. Moreno, and J. Vives. 1984. Direct measurement of antibody affinity distribution by hapten-inhibition enzyme immunoassay. *Mol. Immunol.* 21:537–543.

11. Pearson, L., and R.W. Lightfoot Jr. 1981. Correlation of DNA-anti-DNA association rates with clinical activity in systemic lupus erythematosus (SLE). *J. Immunol.* 126:16–19.

12. Harris, S.L., A.S. Dagtas, and B. Diamond. 2002. Regulating the isotypic and idiotypic profile of an anti–PC antibody response: lessons from peptide mimics. *Mol. Immunol.* 39:263–272.

13. McHeyzer-Williams, L.J., M. Cool, and M.G. McHeyzer-Williams. 2000. Antigen-specific B cell memory: expression and replenishment of a novel b220⁻ memory b cell compartment. *J. Exp. Med.* 191:1149–1166.

14. Manz, R.A., A. Thiel, and A. Radbruch. 1997. Lifetime of plasma cells in the bone marrow. *Nature.* 388:133–134.

15. Slifka, M.K., R. Antia, J.K. Whitmire, and R. Ahmed. 1998. Humoral immunity due to long-lived plasma cells. *Immunity.* 8:363–372.

16. Slifka, M.K., M. Matloubian, and R. Ahmed. 1995. Bone marrow is a major site of long-term antibody production after acute viral infection. *J. Virol.* 69:1895–1902.

17. Jacob, J., R. Kassir, and G. Kelsoe. 1991. In situ studies of the primary immune response to (4-hydroxy-3-nitrophenyl)acetyl. I. The architecture and dynamics of responding cell populations. *J. Exp. Med.* 173:1165–1175.

18. Smith, K.G., T.D. Hewitson, G.J. Nossal, and D.M. Tarlinton. 1996. The phenotype and fate of the antibody-forming cells of the splenic foci. *Eur. J. Immunol.* 26:444–448.

19. McHeyzer-Williams, M.G., M.J. McLean, P.A. Lalor, and G.J. Nossal. 1993. Antigen-driven B cell differentiation in vivo. *J. Exp. Med.* 178: 295–307.

20. Martin, A., and M.D. Scharff. 2002. Somatic hypermutation of the AID transgene in B and non-B cells. *Proc. Natl. Acad. Sci. USA.* 99:12304–12308.

21. Vogel, L.A., L.C. Showe, T.L. Lester, R.M. McNutt, V.H. Van Cleave, and D.W. Metzger. 1996. Direct binding of IL-12 to human and murine B lymphocytes. *Int. Immunol.* 8:1955–1962.

22. Dubois, B., J.M. Bridon, J. Fayette, C. Barthelemy, J. Banchereau, C. Caux, and F. Briere. 1999. Dendritic cells directly modulate B cell growth and differentiation. *J. Leukoc. Biol.* 66:224–230.

23. Dubois, B., C. Massacrier, B. Vanbervliet, J. Fayette, F. Briere, J. Banchereau, and C. Caux. 1998. Critical role of IL-12 in dendritic cell-induced differentiation of naive B lymphocytes. *J. Immunol.* 161:2223–2231.

24. Jacob, C.O., F. Hwang, G.D. Lewis, and A.M. Stall. 1991. Tumor necrosis factor alpha in murine systemic lupus erythematosus disease models: implications for genetic predisposition and immune regulation. *Cytokine.* 3:551–561.

25. O'Connor, B.P., M. Cascalho, and R.J. Noelle. 2002. Short-lived and long-lived bone marrow plasma cells are derived from a novel precursor population. *J. Exp. Med.* 195:737–745.

26. Balazs, M., F. Martin, T. Zhou, and J. Kearney. 2002. Blood dendritic cells interact with splenic marginal zone B cells to initiate T-independent immune responses. *Immunity.* 17:341–352.

27. Metzger, D.W., R.M. McNutt, J.T. Collins, J.M. Buchanan, V.H. Van Cleave, and W.A. Dunnick. 1997. Interleukin-12 acts as an adjuvant for humoral immunity through interferon-gamma-dependent and -independent mechanisms. *Eur. J. Immunol.* 27:1958–1965.

28. Durali, D., M.G. de Goer de Herve, J. Giron-Michel, B. Azzarone, J.F. Delfraissy, and Y. Taoufik. 2003. In human B cells, IL-12 triggers a cascade of molecular events similar to Th1 commitment. *Blood.* 102:4084–4089.

29. Gatto, D., T. Pfister, A. Jegerlehner, S.W. Martin, M. Kopf, and M.F. Bachmann. 2005. Complement receptors regulate differentiation of bone marrow plasma cell precursors expressing transcription factors Blimp-1 and XBP-1. *J. Exp. Med.* 201:993–1005.

30. Grimaldi, C.M., J. Cleary, A.S. Dagtas, D. Moussai, and B. Diamond. 2002. Estrogen alters thresholds for B cell apoptosis and activation. *J. Clin. Invest.* 109:1625–1633.

31. McGaha, T.L., B. Sorrentino, and J.V. Ravetch. 2005. Restoration of tolerance in lupus by targeted inhibitory receptor expression. *Science.* 307:590–593.

32. Nimmerjahn, F., and J.V. Ravetch. 2005. Divergent immunoglobulin g subclass activity through selective Fc receptor binding. *Science.* 310:1510–1512.

33. Schroeder, J.T., A.P. Bieneman, H. Xiao, K.L. Chichester, K. Vasagar, S. Saini, and M.C. Liu. 2005. TLR9- and FcepsilonRI-mediated responses oppose one another in plasmacytoid dendritic cells by down-regulating receptor expression. *J. Immunol.* 175:5724–5731.

34. Park-Min, K.H., N.V. Serbina, W. Yang, X. Ma, G. Krystal, B.G. Neel, S.L. Nutt, X. Hu, and L.B. Ivashkiv. 2007. FcgammaRIII-dependent inhibition of interferon-gamma responses mediates suppressive effects of intravenous immune globulin. *Immunity.* 26:67–78.

35. Laborde, E.A., S. Vanzulli, M. Beigier-Bompadre, M.A. Isturiz, R.A. Ruggiero, M.G. Fourcade, A.C. Catalan Pellet, S. Sozzani, and M. Vulcano. 2007. Immune complexes inhibit differentiation, maturation, and function of human monocyte-derived dendritic cells. *J. Immunol.* 179:673–681.

36. Inaba, K., M. Inaba, N. Romani, H. Aya, M. Deguchi, S. Ikehara, S. Muramatsu, and R.M. Steinman. 1992. Generation of large numbers of dendritic cells from mouse bone marrow cultures supplemented with granulocyte/macrophage colony-stimulating factor. *J. Exp. Med.* 176:1693–1702.

37. Steinman, R.M., G. Kaplan, M.D. Witmer, and Z.A. Cohn. 1979. Identification of a novel cell type in peripheral lymphoid organs of mice. V. Purification of spleen dendritic cells, new surface markers, and maintenance in vitro. *J. Exp. Med.* 149:1–16.

38. Bardwell, P.D., A. Martin, E. Wong, Z. Li, W. Edelmann, and M.D. Scharff. 2003. Cutting edge: the G-U mismatch glycosylase methyl-CpG binding domain 4 is dispensable for somatic hypermutation and class switch recombination. *J. Immunol.* 170:1620–1624.